

Carbon Dioxide Reforming of Alcohols on Porous Membrane Catalyst Systems

M. V. Tsodikov^a, A. S. Fedotov^a, V. V. Zhmakin^a, K. B. Golubev^a, V. N. Korchak^b, V. N. Bychkov^b,
N. Yu. Kozitsyna^c, and I. I. Moiseev^a

^a Topchiev Institute of Petrochemical Synthesis, Russian Academy of Sciences, Moscow

^b Semenov Institute of Chemical Physics, Russian Academy of Sciences, Moscow

^c Kurnakov Institute of General and Inorganic Chemistry, Russian Academy of Sciences, Moscow

Received December 16, 2010

Abstract—The features of the carbon dioxide reforming of ethanol and an ethanol–glycerol mixture to synthesis gas in the presence of porous membrane catalyst systems have been studied. It has been shown that the CO₂ reforming of alcohols in open pores of ceramic membranes modified with nanosized active palladium-containing components proceeds at a higher rate as compared to that in a conventional fixed-bed flow reactor charged with a catalyst of similar composition.

DOI: 10.1134/S0965544111070127

The use of the products derived from biomass, which is renewable raw material, as feedstock for manufacturing energy carriers is of great significance for the power engineering and chemical industries [1, 2]. The main products obtainable from biomass and possessing a high potential as an alternative source of hydrocarbons are ethanol and glycerol. It has been shown that noble metals are promising catalysts for the steam conversion of ethanol [3, 4].

It should be noted that the development of processes for CO₂ conversion of these substrates into synthesis gas is extremely important because it allows for utilization of carbon dioxide, which is a greenhouse gas, as an additional source of carbon-containing feedstock. However, only few works are known in this field [5–7]. In those works, the conversion of alcohols was carried out in a conventional reactor with a fixed catalyst bed at temperatures of 750–900°C.

Earlier, it was shown that gas phase reactions of stable molecules, such as carbon dioxide and methane, are significantly intensified when porous membrane catalyst systems are used [8–10].

In this paper, we present the results of the carbon dioxide conversion of ethanol and ethanol–glycerol mixtures that proceeds in the microchannels of porous ceramic membranes modified with a small amount of nanosize palladium-containing mono- and bimetallic catalysts.

EXPERIMENTAL

Porous membrane supports prepared by self-propagating high-temperature synthesis (SHS) were used in the study [11].

In order to increase the specific surface area and decrease the pore size, first, a buffer porous TiO₂ coating was formed from a tetraethoxytitanium colloid solution on the inner surface of the channels. Then palladium-containing catalytic components were deposited onto the porous titanium dioxide by means of the alkoxy method based on tetrabytoxytitanium colloid solutions dissolved together with mono- and heteronuclear palladium-containing acetate complexes, which are used as precursors and are described in [12, 13]. The catalysts preparation procedure was detailed in [14]. The bimetallic palladium-containing Pd–Co and Pd–Zn systems and Pd systems were prepared so that they had the composition as specified in the table.

The carbon dioxide reforming of ethanol and an ethanol–glycerol mixture were studied under the following conditions: a temperature of 250–650°C, an inlet reactor pressure of 1–5 atm, an outlet reactor pressure of 1 atm, a flow rate of liquid substrates (supplied from a liquid feeder) of 0.5–3 ml/min, and a gas–vapor mixture space velocity of 12500 h⁻¹. A gaseous feed mixture consisting of alcohol vapor and CO₂, taken in a CO₂/substrate ratio of 5 : 1, after a pre-

Composition and amount of active components on the membrane catalyst systems

Catalyst system	Concentration of active components		
	Pd, wt %	Co, wt %	Zn, wt %
1 Pd	0.023	–	–
2 Pd–Co	0.018	0.009	–
3 Pd–Zn	0.023	–	0.011

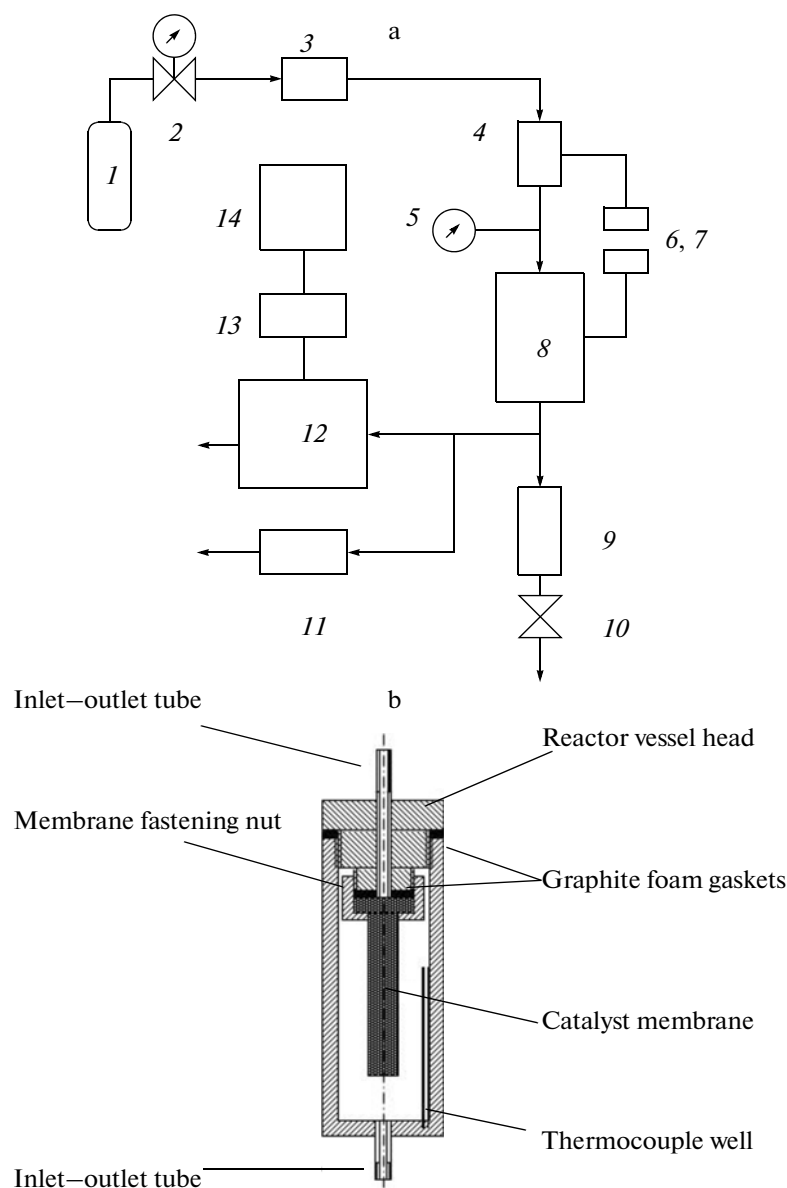


Fig. 1. (a) Flow diagram of the membrane catalytic bench unit; and (b) schematic of the membrane reactor; (1) feed gas mixture, (2) pressure reducer, (3) gas flow meter, (4) preheating oven, (5) pressure gauge, (6, 7) thermocouples, (8) unique heated membrane reactor (Scheme 2), (9) receiver for liquid, (10) shutoff valve, (11) CO and CO₂ analyzer, (12) chromatograph, (13) analog-to-digital converter, and (14) computer.

heater, was fed to the outer side of the membrane at a certain temperature. After the reactor, the liquid phase was separated from the gas phase at the separator/condenser and fed to a receiver. The gas phase was analyzed on-line. The flow chart of the process and the membrane reactor are shown in Figs. 1a and 1b, respectively.

In order to compare the efficiency of CO₂ reforming of ethanol on a porous membrane, the process was also carried out in a conventional fixed-bed flow reactor. The catalyst bed of the reactor was made of grains 3–4 mm in size obtained by crushing of the membrane catalyst system. The ethanol vapor and

carbon dioxide reactant mixture was fed to the bottom, and the products were sampled for analysis from the top of the reactor.

The products were analyzed on a CHROM5 chromatograph with a thermal conductivity detector, using high-purity argon (argon content at least 99.998 vol %, TU (Technical Specifications) 6-21-12-94) as the carrier gas at a flow rate of 30 ml/min. A chromatographic column 1 m × 3 mm in size was packed with SKT brand activated carbon (0.2–0.3 mm). The CO and CO₂ concentrations were also determined by IR spectroscopy using Riken Keiki RI-550A sensors.

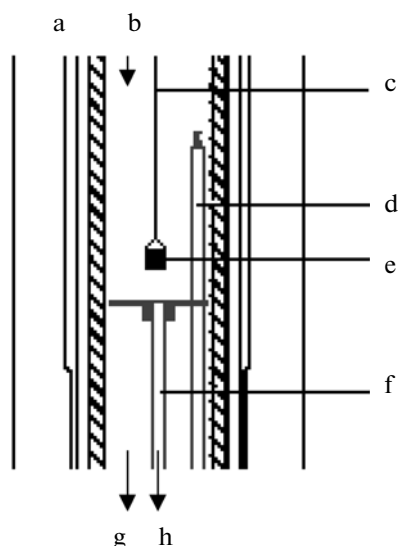


Fig. 2. Schematic of the thermogravimetric cell: (a) oven, (b) feed gas mixture inlet, (c) quartz filament, (d) thermocouple, (e) suspended pan with a specimen, and (f) aluminum capillary for sampling the gas mixture after the specimen to analyze in a mass spectrometer.

The dynamics of the CO_2 methane reforming (CMR) process on the membrane catalyst system (MCS) was studied on a precision unit including a gravimetric cell (Fig. 2), a high-precision thermobalance, and a mass spectrometer.

The interaction of the catalysts separately with ethanol vapor and carbon dioxide was studied in a setup that included a SETSYS EVOLUTION thermobalance (Setaram) and an OmniStar mass spectrometer (Pfeiffer). A helium flow was passed at a rate of 20 ml/min through a bubbler with ice-cooled ethanol (0°C). Then the flow with the alcohol vapor was sent to the thermobalance via the auxiliary gas line. Simultaneously, a flow of pure helium (40 ml/min) was supplied to the thermobalance through the main line. These two streams were intermixed at the top of the tubular oven of the thermobalance, and the mixed stream arrived at the specimen placed in a quartz cup, suspended in the middle of the thermobalance tubular oven. The portion of the stream that came in contact with the specimen was directed to the mass spectrometer through a heated capillary.

The sequence of experimental operations was as follows: (1) heating in He-carried ethanol vapor from 30 to 500°C at a rate of 10°C , holding at 500°C for 1800 s, then pumping-out of the gas phase and cooling to 30°C ; (2) heating in a pure CO_2 flow (20 ml/min) from 30 to 700°C at a rate of 10°C , holding at 700°C for 600 s, and cooling; (3) reheating in ethanol vapor in He from 30 to 500°C at a rate of 10°C , holding at 500°C for 1800 s, then, pumping-out of the gas phase and cooling to 30°C ; (4) heating in a 20 ml/min flow

of pure CO_2 from 30 to 700°C at a rate of 10°C ; and (5) holding at 700°C for 600 s and cooling.

The change in the gas phase composition was monitored by recording mass-spectrometer ion currents at $m/z = 2$ (H_2), 18 (H_2O), 28 (CO), 29 (acetaldehyde + $\text{C}_2\text{H}_5\text{OH}$), 31 ($\text{C}_2\text{H}_5\text{OH}$), and 44 (acetaldehyde + CO_2).

RESULTS AND DISCUSSION

Carbon Dioxide Reforming of Ethanol

The carbon dioxide reforming of ethanol proceeds intensively on the membrane catalyst system (MCS) to form the synthesis gas. The almost complete conversion is attained at 500°C on any of the catalysts used (Fig. 3).

However, a nearly 100% yield of hydrogen is achieved on the Pd-Co-containing MCS at 650°C (Fig. 4). A decrease in the hydrogen yield in the presence of the Pd- and Pd-Zn-containing systems was caused by the formation of methane along with the synthesis gas. It is also seen from Figs. 3 and 4 that the ethanol conversion and the hydrogen yield on the membrane catalyst systems are substantially higher than those of the process run in the conventional flow reactor with a fixed bed of the grained catalyst.

It is seen from Fig. 4 that the process proceeds more actively in the presence of the Pd-Co catalyst system distributed on the inner surface of membrane channels than in the flow reactor with a fixed bed of the same catalyst prepared by crushing of the membrane. The membrane itself, made from a Ni-Al alloy, exhibits activity in the carbon dioxide reforming of ethanol.

The deposition of a small amount of catalyst markedly increases MCS activity, mainly in the low-temperature region. For example, the process is initiated on the MCS at a temperature of approximately 100°C below that in the presence of the initial membrane, as we can see from Fig. 5. Unlike the case of carbon dioxide methane reforming in which the presence of a catalyst increases the activity by an order of magnitude within the entire range of temperatures examined, the difference in the conversion rate of ethanol as a more reactive chemical is slightly leveled with an increase in temperature to 650°C (15).

The dependence of the specific yield of the products of carbon dioxide ethanol reforming upon the space time is shown in Fig. 6. It is seen from Fig. 6 that the total synthesis gas yield at 650°C in the presence of the [Pd-Co] catalyst is $16000 \text{ l}/(\text{dm}^3_{\text{membrane}} \text{ h})$ over a space time of 0.16 s.

This activity is substantially higher than that ever displayed by the relevant catalysts in the conventional fixed-bed reactor [5–7].

The composition of gaseous products at an ethanol space velocity of 12500 h^{-1} is presented in Fig. 7.

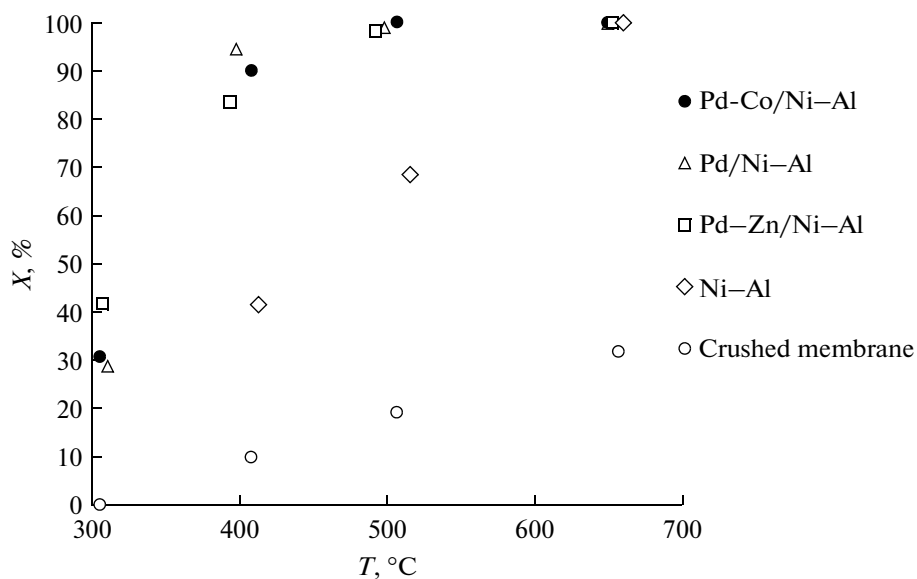


Fig. 3. Plot of the ethanol conversion during carbon dioxide reforming on the membrane catalyst systems modified with different Pd-containing catalysts. Abscissa axis, temperature, °C. Ordinate axis, conversion, vol %.

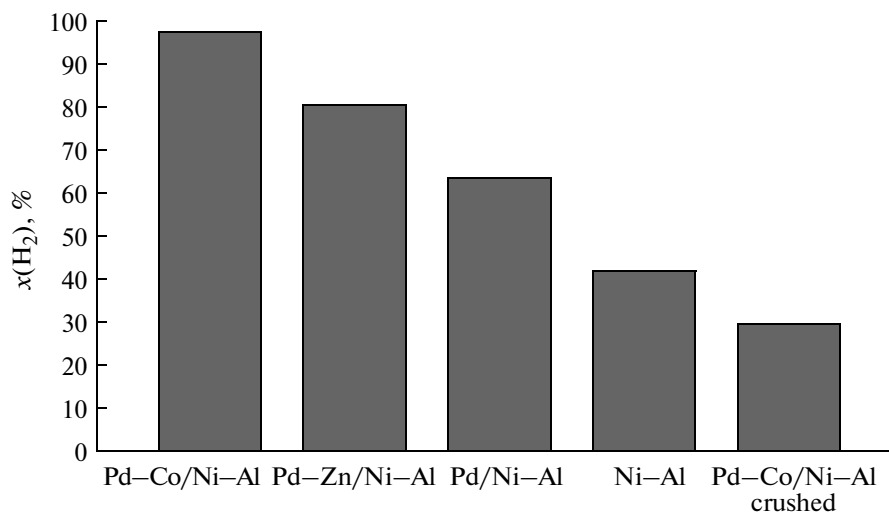
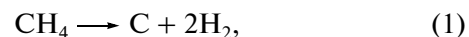


Fig. 4. Yield of hydrogen on various membrane catalyst systems and on the crushed membrane ($T = 650^{\circ}\text{C}$, $V = 12500 \text{ h}^{-1}$). Abscissa axis, membrane type. Ordinate axis, hydrogen yield, vol %.

It is seen from Fig. 7 that the amount of carbon monoxide and hydrogen increases as the amount of carbon dioxide decreases during the conversion. The methane content of the gaseous products passes through a maximum at $450\text{--}500^{\circ}\text{C}$ and then drops to become insignificant at 650°C . The gases contain only traces of ethylene.

These data suggest that the methane produced in the process experiences conversion at a temperature above 500°C into the synthesis gas via the known route determined in [8–10]:



To study the dynamics of CO_2 ethanol reforming, the process was studied step by step on a unit equipped with a high-sensitivity balance and a mass-spectrometric analyzer in the temperature-programming mode. As is seen from Fig. 8, which presents the thermogravimetric data on heating of a fresh specimen of the crushed catalytic membrane containing the Pd-Co catalyst system in an ethanol vapor-free stream, there are three regions of mass change.

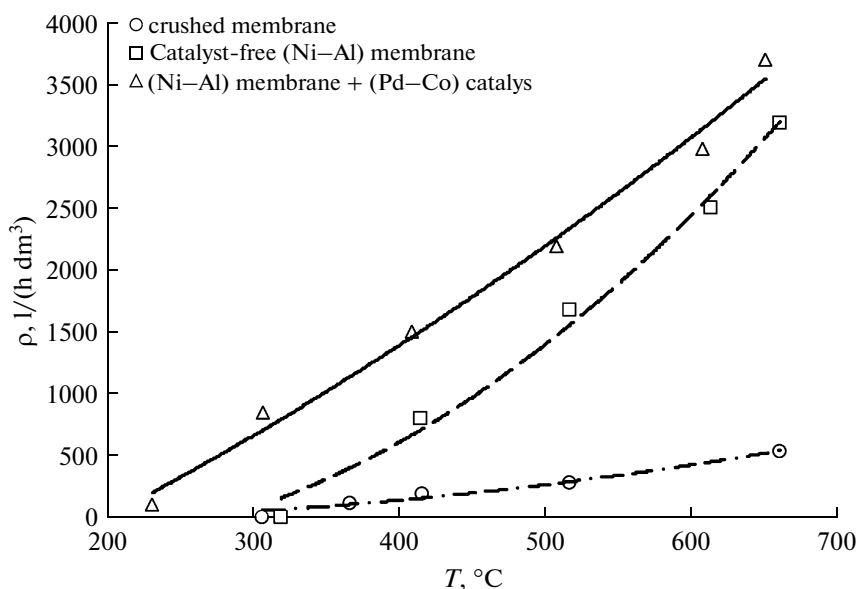


Fig. 5. Activity of the initial membrane, the membrane catalyst system, and the grained catalyst at different temperatures. Abscissa axis, temperature, °C. Ordinate axis, syngas formation rate, $l/(dm^3_{\text{membrane}} \cdot h)$.

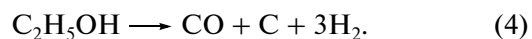
The mass of a specimen decreases over the temperature range of 300–350°C followed by its increase within the range of 350–450°C and a subsequent dramatic drop until 500°C.

Within the temperature range of 300–400°C, the ethanol concentration decreases and H_2 and acetaldehyde are produced. A relatively small amount of carbon monoxide ($m/z = 28$) forms under these conditions (Fig. 9). These products indicate that the ethanol dehydrogenation reaction occurs:



Within the temperature range of 400–470°C, the intense formation of H_2 and CO is observed against the

background of a dramatic decrease in ethanol concentration. The catalyst weight rapidly rises, thereby indicating carbon deposition onto the catalyst. Thus, the following overall reaction takes place during this interval:



The simultaneous decrease in the acetaldehyde concentration suggests that acetaldehyde formation reaction (3) is intermediate in the mechanism of overall reaction (4), which can be represented as the following final steps:

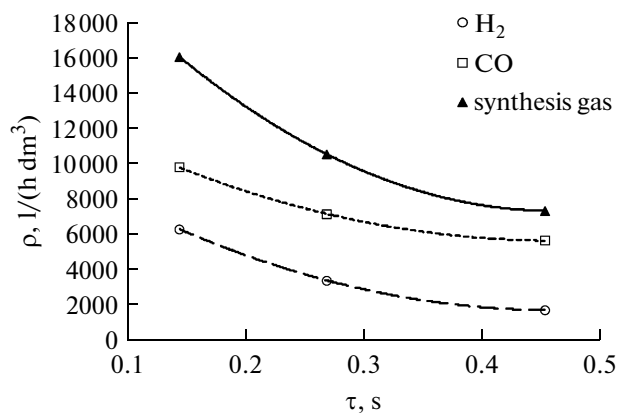
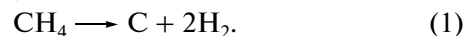
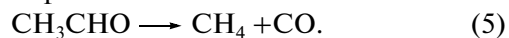


Fig. 6. Dependence of the specific synthesis gas yield on the space time (Pd-Co catalyst; $T = 650^\circ\text{C}$). Abscissa axis, space time, s. Ordinate axis, specific synthesis gas yield, $l/(dm^3_{\text{membrane}} \cdot h)$.

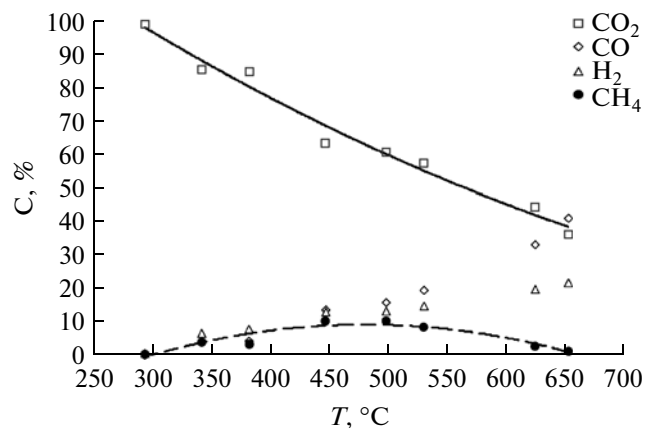


Fig. 7. Product composition of carbon dioxide ethanol reforming at different temperatures (Pd-Co catalyst; $V = 12500 \text{ h}^{-1}$). Abscissa axis, temperature, °C. Ordinate axis, amount, vol %.

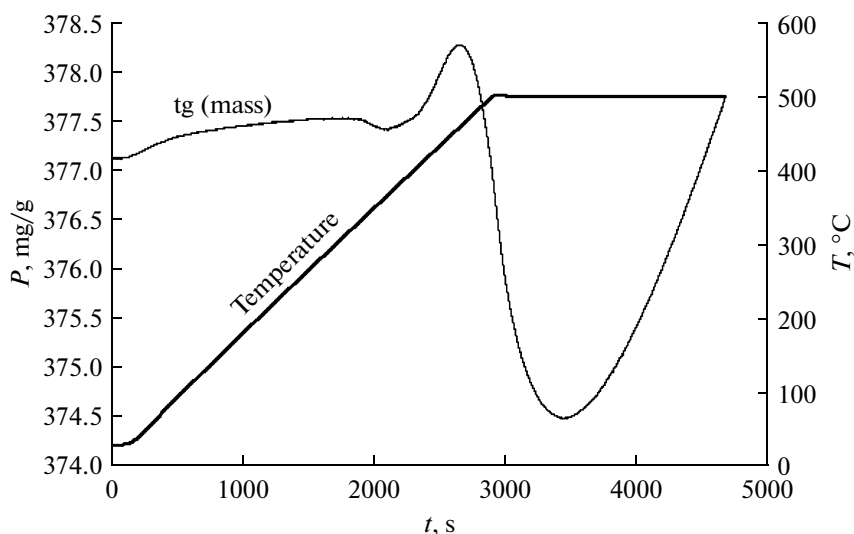
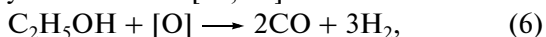


Fig. 8. Thermogravimetric analysis data for a fresh specimen of the crushed catalytic membrane containing the Pd–Co catalyst system, as heated in the programmed-temperature mode (carrier gas is He containing ethanol vapor). Abscissa axis, time, s. Ordinate axes, mass of specimen P , mg/g (left) and temperature, T , °C (right).

As is seen from Fig. 7, it is in this temperature range that methane appears in the gas phase. At temperatures above 450°C, methane intensely dissociates at the surface of catalytic microchannels of the membrane to form hydrogen and carbon, as shown in [8–10, 15].

The further heating of the specimen to 500°C leads to a sharp drop in the catalyst mass and the subsequent increase in mass, which continues until the end of the experiment. The mass loss is accompanied by a peak in the curve at $m/z = 44$, which indicates the formation of CO_2 . The presence of carbon monoxide and carbon dioxide at this stage is an indication of possible partial and deep oxidation of ethanol by oxygen of the membrane oxide phases identified by electron microscopy and X-ray diffraction in [15, 16]:



The conclusion that it is the carbon deposition that is responsible for the increase in mass of the catalyst during its interaction with ethanol vapor is confirmed by the results of the subsequent treatment of the specimen with carbon dioxide leading to the formation of CO according to reaction (2) (Fig. 10). The catalyst mass loss is observed in these experiments, which is accompanied by the formation of CO due to reaction (2).

Carbon is almost completely removed in this stage, since the system begins to operate in the steady-state mode at a temperature of 500°C.

Figure 11 presents the logarithmic hydrogen generation rate plotted against the inverse temperature. The linear character of the plots indicates the absence of diffusion constraints during the process in the micropore channels of both initial and catalyst-modi-

fied membranes. It also follows from the given data that the activation parameter of the hydrogen formation process drops practically twice if it proceeds on the membrane modified with the catalyst system.

When the process is run in the fixed-bed flow reactor with the catalyst prepared by crushing the MCS, the activation parameter remains the same. However, the preexponential factor drops by a factor of almost three in comparison with that for the process on the MCS (Fig. 11). It is known that the preexponential factor reflects the accessibility of the active surface of the catalyst system to substrate molecules [17–19]. This result also agrees with the data earlier obtained in [20].

These results confirm the previous conclusions on the accessibility of the active surface to substrate molecules and, probably, quite rapid desorption of reaction products from catalytically active centers.

Earlier, based on the results of theoretical analysis of the diffusion mechanism in porous membrane microchannels modified with dispersed catalyst particles in terms of independent models of diffusion, we assumed that the probability of transversal diffusion increases, and this, as the pore size decreases, can lead to anisotropy in both the permeability of gas substrates and the membrane catalytic properties, depending on the direction of a transmembrane flow [21].

It can be assumed from the results that the increase in the preexponential factor is an indication of a significant increase in the statistical number of collisions of substrate molecules with catalytically active centers in the inner space of channels of the membrane modified with particles of the catalyst system with quite a large pore size of 1–3 μm , when the process is run in the membrane filtration mode, thereby

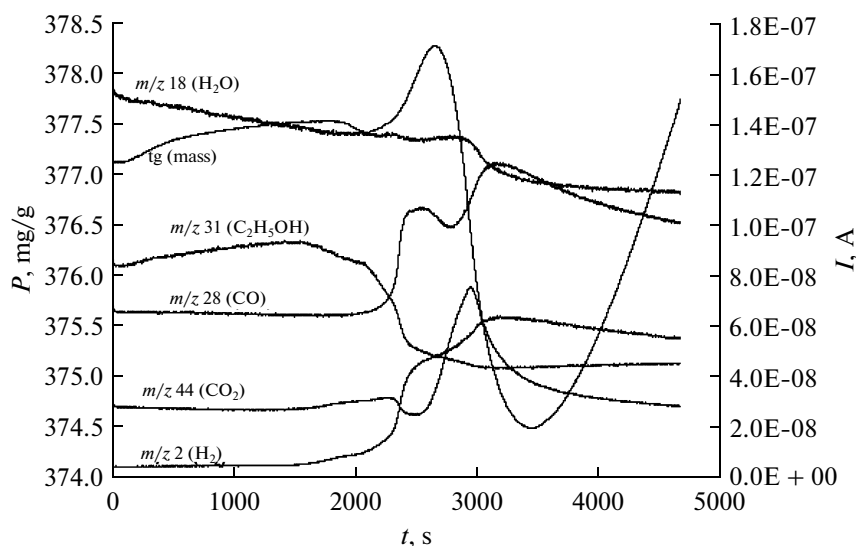


Fig. 9. Thermogravimetric data for a specimen of the crushed membrane containing the Pd–Co catalyst system and mass-spectrometric data for the ethanol conversion products. Abscissa axis, time, s. Ordinate axis, specimen mass, P , mg/g (left); ion current, A (right).

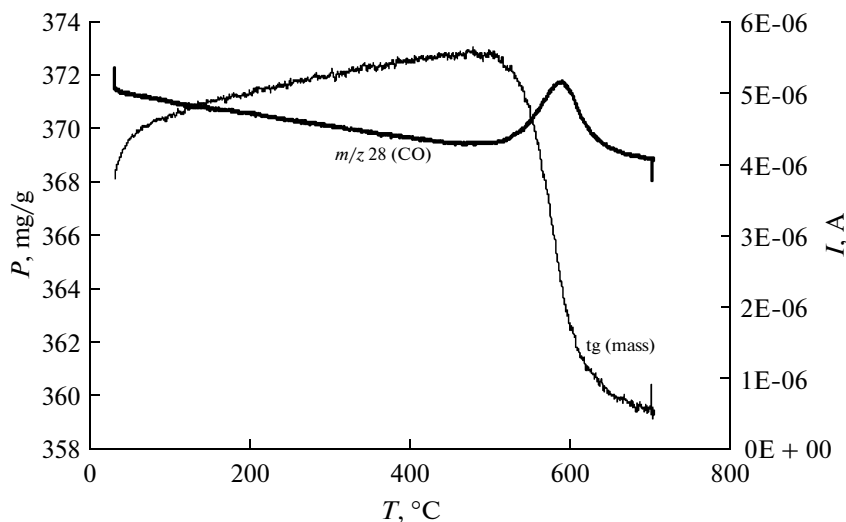


Fig. 10. Thermogravimetric data for the specimen and mass-spectrometric data for the products formed during CO_2 passing through the crushed catalytic membranes after the ethanol conversion step. Abscissa axis, temperature, T , $^\circ\text{C}$. Ordinate axis, specimen mass, P , mg/g (left); ion current, A (right).

leading to a marked increase in the rate of CO_2 reforming of ethanol.

Carbon Dioxide Reforming of an Ethanol–Glycerol Mixture

In connection with the prospect of manufacturing biodiesel fuel from renewable raw materials, the prob-

lem of utilizing expectedly large amounts of released glycerol arises. The production of hydrogen-containing gas from glycerol can be one of the solutions to this problem. In this context, we studied the conversion of glycerol in a mixture with ethanol during the carbon dioxide reforming process with the use of membrane catalyst systems. It might be expected that in the processing of the mixture, the yield of the synthesis gas

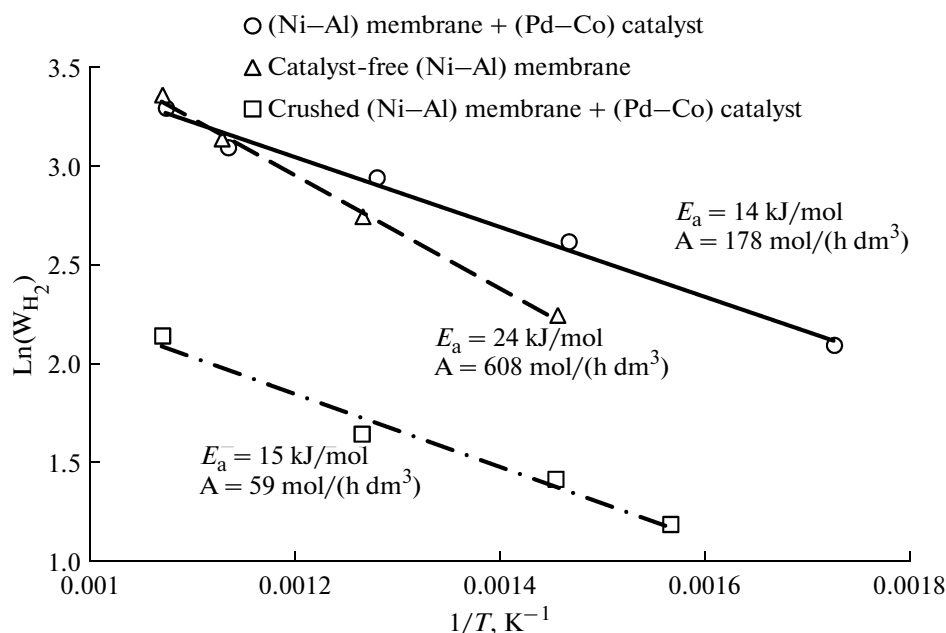
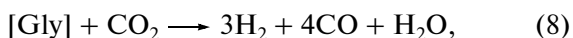


Fig. 11. Arrhenius plot of the hydrogen formation rate. Abscissa axis, $\ln W, 1/(\text{dm}^3_{\text{membrane}} \text{ h})$. Ordinate axis, inverse temperature, $1/T, \text{K}^{-1}$.

components during carbon dioxide reforming of the glycerol-containing mixture would be greater by one mole of CO compared with ethanol conversion, as follows from reactions (8) and (9):

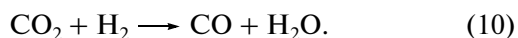


The data on the conversion of the ethanol–glycerol mixture are presented in Fig. 12. They show that the Pd–Co-containing system exhibits the highest activity, as in the case of ethanol conversion, allowing the initial mixture to be almost completely converted at 650°C.

The specific yield of synthesis gas is $20000 \text{ l}/(\text{dm}^3_{\text{membrane}} \text{ h})$ (Fig. 13). As is seen from Fig. 13, the gas composition significantly varies depending on the space time.

When the space time is 0.35 s, the amount of CO formed is almost three times the hydrogen yield, whereas their concentrations are about the same at 0.1 s.

Earlier it has been shown that the increasing space time in CO_2 methane reforming leads to an increase in the contribution of the CO_2 hydrogenation reaction, the so-called reverse water gas shift reaction [15]:



Most likely, the active Pd–Co-containing components exhibit a high activity in the hydrogenation reaction, leading to an increase in the CO_2 reduction depth with the increasing space time.

CONCLUSIONS

The membrane catalyst system containing a small amount of active Pd–Co-containing components within the inner volume shows a high activity in the carbon dioxide conversion of ethanol and the ethanol–glycerol mixture, which are the main products derived from biomass. The total conversion of these substrates is attained with an amount of the active components almost an order of magnitude lower in comparison to the palladium-containing, steam ethanol-reforming catalysts loaded into the conventional flow reactor [3, 5–7]. It has been shown [15, 16] that

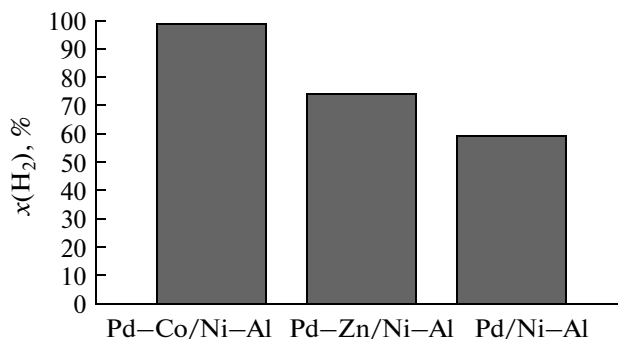


Fig. 12. Dependence of the CO_2 conversion of the ethanol–glycerol mixture on the temperature of the process in the presence of palladium-containing catalysts. Abscissa axis, MCS composition. Ordinate axis, yield of synthesis gas on a converted ethanol basis, vol %.

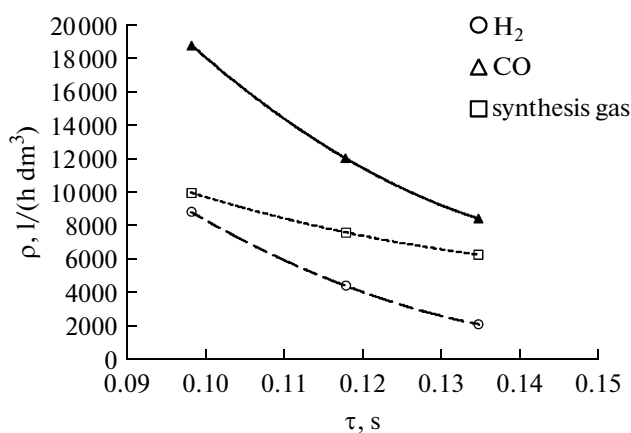


Fig. 13. Dependence of the specific yield of synthesis gas during the CO₂ reforming of the ethanol–glycerol mixture on the space time (Pd–Co catalyst; $T = 650^\circ\text{C}$). Abscissa axis, space time, s. Ordinate axis, specific yield of synthesis gas, $l/(dm^3_{\text{membrane}} \text{ h})$.

the catalyst systems formed on the inner pore surface of the membrane support are nanoparticles of 15–20 nm in size (d) uniformly distributed over the surface. The studied transformations of the substrates are endothermic processes. Their enhancement in catalytic membrane microchannels is probably caused by the increased active surface area of the nanosized catalyst components and improved parameters of mass and heat transfer in the inner space of open membrane pores, as noted in many published papers [22, 23]. According to the transmission electron microscopy and temperature-programmed reduction data discussed in [24], the Pd–Co-containing system consists of nanosized Pd and Co metal clusters distributed near to the oxide phases of the mixed cobalt oxide $x\text{CoO} \cdot y\text{Co}_2\text{O}_3$ having the spinel structure. The bifunctional properties of such a system are probably responsible for the high activity in the redox reactions that proceed during the carbon dioxide conversion of ethanol and the ethanol–glycerol mixture. The deposition the active components from metal complex precursors containing both palladium and cobalt atoms in the same structure presumably promotes the formation of active centers in immediate proximity to one another on the surface, thereby facilitating the access of the substrates and, hence, enhancing the catalytic activity.

ACKNOWLEDGMENTS

This work was supported by the Russian Foundation for Basic Research, project nos. 10-03-00715 and 09-03-12060.

REFERENCES

1. D. Charles, *Science (Biofuels)* **324**, 587 (2009).
2. S. D. Varfolomeev, I. I. Moiseev, and B. F. Myasoedov, *Vestn. Akad. Nauk* **79**, 595 (2009).
3. A. C. Basagianinis, P. Panagiotopoulou, and X. E. Verykios, *Top. Catal.* **51**, 2 (2008).
4. M. Scott, M. Goeffroy, W. Chiu, et al., *Top. Catal.* **51**, 13 (2008).
5. K. J. Puolakka and A. O. I. Krause, *Catal. Lett.* **116**, 87 (2007).
6. Wang Xiaodong, Li Maoshuai, Wang Meihua, et al., *Fuel* **88**, 2148 (2009).
7. A. J. Akande, R. O. Idem, and A. K. Dalai, *Appl. Catal. A: Gen.* **287**, 159 (2005).
8. V. Teplyakov, M. Tsodikov, M. Magsumov, et al., *Eurumembrane Desalination*, 1–3 (2006).
9. A. G. Dedov, A. S. Loktev, K. V. Parkhomenko, et al., *Khim. Tekhnol.*, No. 5, 208 (2008).
10. V. Zhmakin, A. Fedotov, V. Teplyakov, et al., *PERMEA2009* (Prague, 2009), Book of abstracts, p. 197.
11. V. I. Uvarov, I. P. Borovinskaya, and A. G. Merzhanov, *RU Patent No. 2175904*, (2000).
12. N. Yu. Kozitsyna, S. E. Nefedov, F. M. Dolgushin, et al., *Inorg. Chim. Acta* **359**, 2072 (2006).
13. N. S. Akhmadullina, N. V. Cherkashina, N. Yu. Kozitsyna, et al., *Inorg. Chim. Acta* **362**, 1943, (2009).
14. M. I. Magsumov, F. S. Fedotov, M. V. Tsodikov, et al., *Russ. Nanotekhnol.* **1**, 142 (2006).
15. A. S. Fedotov, V. V. Teplyakov, M. V. Tsodikov, et al., *ICCMR9*, Lion, 2009, Book of abstracts, p. 163.
16. A. Fedotov, V. Zhmakin, M. Tsodikov, and I. Moiseev, in *Proceedings of First Workshop of COST Action, CM0903 "Utilization of Biomass for Sustainable Fuels and Chemicals (UBIOCHEM)"*, Spain, 2010.
17. S. Z. Roginskii, *Probl. Kinet. Katal.* **6**, 9 (1944).
18. S. Z. Roginskii, *Heterogeneous Catalysis in Chemical Industry* (GNTIKhL, Moscow, 1955) [in Russian].
19. O. M. Poltorak, *Lectures on the Theory of Catalysis* (Mosk. Univ., Moscow, 1968) [in Russian].
20. M. V. Tsodikov, N. I. Laguntsov, M. I. Magsumov, et al., *Izv. Akad. Nauk, Ser. Khim.*, No. 9, 6 (2004).
21. I. M. Kurchatov, N. I. Laguntsov, M. V. Tsodikov, A. S. Fedotov, et al., *Kinet. Katal.* **39**, 120 (2008).
22. A. A. Khasin, *Russ. Zh. Khim. Ob-va im. D.I. Mendeleeva* **47**, 36 (2003).
23. F. Kaptejn, J. J. Heiszwolf, T. A. Nijhuis, and J. A. Moulijn, *Ind. Catal.* **3**, 24 (1999).
24. V. Zhmakin, A. Fedotov, V. Uvarov, et al., in *Proceedings of Second German–Russian Seminar on Catalysis "Bridging the Gap between Model and Real Catalysis"*, Closter Seeon, 2010.